BULLETIN OF THE EARTHQUAKE
RESEARCH INSTITUTE
Vol. 42 (1964), pp. 407-425

20. *Propagation of Spheroidal Disturbances on an Elastic Sphere with a Homogeneous Mantle and a Core*

By Yasuo SATÔ and Tatsuo USAMI,

Earthquake Research Institute.

(Read July 14, 1964.—Received July 30, 1964.)

Abstract

Propagation of spheroidal disturbances on an elastic sphere with a homogeneous mantle and a liquid core was studied using the method of superposition of various normal mode oscillations.

The theoretical seismograms thus obtained show similar characteristics with our previous study on a homogeneous sphere, the main features found in the present study being as follows:

1) Free oscillation periods show different features from the case of a homogeneous sphere. Moreover, there exists an extra branch which lies between the fundamental and first higher modes of the case of a homogeneous sphere. This is a kind of boundary waves between two media, the mantle and the core.

2) The phase and group velocities become very complicated by the existence of a core.

3) Reflected phase at the core-mantle boundary are found in theoretical seismograms.

4) Transmitted waves through the liquid core are also seen in the seismograms.

5) Diffracted waves in the shadow zone can also be traced.

1. Introduction

The problem of the synthesis of theoretical seismograms has been studied for the past few years and the propagation of the torsional disturbances was calculated for a homogeneous elastic sphere[1] and also for a model with a homogeneous mantle and a liquid core[2], assuming a localized instantaneous stress on the surface. A similar problem of the propagation of spheroidal oscillations was solved recently for a homogeneous model (case I))[3]. In the present study, however, as a natural development of the above work, a homogeneous mantle and a

liquid core was assumed and the problem was solved in a similar way (case II)). A considerable difference from the case of a homogeneous sphere is found in the free oscillation period. The amount of discrepancy is not always very large, but the velocity deduced thereof, especially the group velocity, is considerably different from the case of a simple sphere. One remarkable fact is the existence of an extra branch that lies between the fundamental and the first higher modes in case I). This branch proves to be a boundary wave between the mantle and the core. The effect of the core can also be found in the phases of body waves, namely the reflected wave at the mantle-core boundary, the transmitted wave through the liquid core and the diffracted wave in the shadow zone.

2. Glossary

Case I) : The problem of a homogeneous sphere
Case II) : The problem of a homogeneous mantle and a homogeneous liquid core
a : radius of the sphere
b : radius of the core
C : phase velocity
C_{mn}, C_{mn}' : coefficient of spherical surface harmonics determined by the geographical distribution of the force applied
$E=0$: frequency equation of the free spheroidal oscillation
$f(t)$: time function of the applied force
$f^*(p)$: Fourier transform of the function $f(t)$
i : radial mode number
j : unit of imaginary number
m : degree of an associated Legendre function
n : order of an associated Legendre function (colatitudinal mode number)
p : frequency
PCP : P wave diffracted in the shadow zone by the core
(r, θ, φ) : polar coordinates
${}_iS_n^u$, ${}_iS_n^v$: common spectrum of radial and colatitudinal components of disturbance
t : time
U : group velocity
$U_n(r)$, $V_n(r)$: distribution function of radial and colatitudinal components of displacement in radial direction

u, v, w : radial, colatitudinal and azimuthal components of displacement respectively

$u(p), v(p), w(p)$: radial, colatitudinal and azimuthal components of displacement in the frequency domain

$({}_iu_n)$: $\sum_{i=1}^{i}\sum_{n=0}^{n} {}_iu_n$

$({}_iv_n)$: $\sum_{i=1}^{i}\sum_{n=0}^{n} {}_iv_n$

V_{s0}, V_{p0} : velocity of shear and dilatational waves in the mantle

V_{pi} : sound wave velocity in the core

η : non-dimensional frequency $(=k_0\cdot a=pa/V_{s0})$

ρ_0, ρ_i : density of mantle and core respectively

3. Fundamental expression

The fundamental procedure is the same for any arbitrary earth's model with radial heterogeneity. Namely the displacements are expressed in the form

$$(u, v, w)=\frac{1}{2\pi}\int_{-\infty}^{\infty}(u(p), v(p), w(p))\cdot\exp(jpt)dp\,, \tag{3.1}$$

in which

$$\begin{aligned}
u(p)&=\sum_{m,n}(U_n(r)/E)\cdot P_n^m(\cos\theta)\cdot(C_{mn}\cos m\varphi+C'_{mn}\sin m\varphi)\cdot f^*(p)\,,\\
v(p)&=\sum_{m,n}(V_n(r)/E)\cdot\frac{d}{d\theta}P_n^m(\cos\theta)\cdot(C_{mn}\cos m\varphi+C'_{mn}\sin m\varphi)\cdot f^*(p)\,,\\
w(p)&=\sum_{m,n}m(V_n(r)/E)\cdot\frac{P_n^m(\cos\theta)}{\sin\theta}\cdot(-C_{mn}\sin m\varphi+C'_{mn}\cos m\varphi)\cdot f^*(p)\,,
\end{aligned} \tag{3.2}$$

$U_n(r)$, $V_n(r)$ are functions determined by the radial distribution of material. When the earth's model is a simple one we can solve the problem analytically and obtain an explicit form of $U_n(r)$ and $V_n(r)$. If, however, the material has a complicated heterogeneous structure the solution can be obtained only numerically. $E(p)=0$ is the characteristic equation for this earth's model. C_{mn} and C'_{mn} are the coefficients of spherical surface harmonics determined by the geographical distribution of the applied force, and $f^*(p)$ is the Fourier transform of the time function at the source.

Using the method of contour integration u and v are expressed in the form

$$u=\frac{j}{2}\sum_{m,n,i}P_n^m(\cos\theta)\cdot(C_{mn}\cos m\varphi+C'_{mn}\sin m\varphi)\cdot\left[\frac{U_n(r)}{dE/dp}\cdot f^*(p)\cdot\exp(jpt)\right]_{p={}_ip_n},$$

$$v=\frac{j}{2}\sum_{m,n,i}\frac{d}{d\theta}P_n^m(\cos\theta)\cdot(C_{mn}\cos m\varphi+C'_{mn}\sin m\varphi)\cdot\left[\frac{V_n(r)}{dE/dp}\cdot f^*(p)\cdot\exp(jpt)\right]_{p={}_ip_n}, \tag{3.3}$$

where ${}_ip_n$ is the root of frequency equation $E=0$ and i is the radial mode number. w has a similar form of expression. In the present study, the effect of gravity is neglected.

4. Non-dimensional frequency of oscillation.

The non-dimensional frequency $k_0a(=pa/V_{s0})$ is calculated and is given in Fig. 1 in the form of continuous curves. Numerical values assumed in the present calculation (case II)) are

$a=6370$ km, $b=(6370-2900)$ km,
$\rho_i/\rho_0=2.2$
$V_{p0}=11.55$ km/sec, $V_{s0}=6.667$ km/sec$=V_{p0}/\sqrt{3}$
$V_{pi}=10.00$ km/sec.

There is an extra branch between the fundamental mode and that which used to be the first higher mode in the problem of a homogeneous sphere (case I)). For convenience, $i=1'$ is given as the radial mode number of this branch. The discrepancy of frequencies between the two cases I) and II) is large when n is small and i is large. As is physically expected, the curve for the present case tends to that for case I) as n tends to ∞. This tendency is slow for larger value of i.

5. Phase and group velocities.

Phase and group velocities are calculated using ordinary asymptotic formulae, namely

$$C=V_{s0}\cdot\gamma/(n+1/2), \tag{5.1}$$

and

$$U=V_{s0}\cdot d\gamma/dn, \tag{5.2}$$

Curves are shown in Fig. 2. To show the features of the group velocity curve in more detail, a part of the figure is enlarged along the abscissa

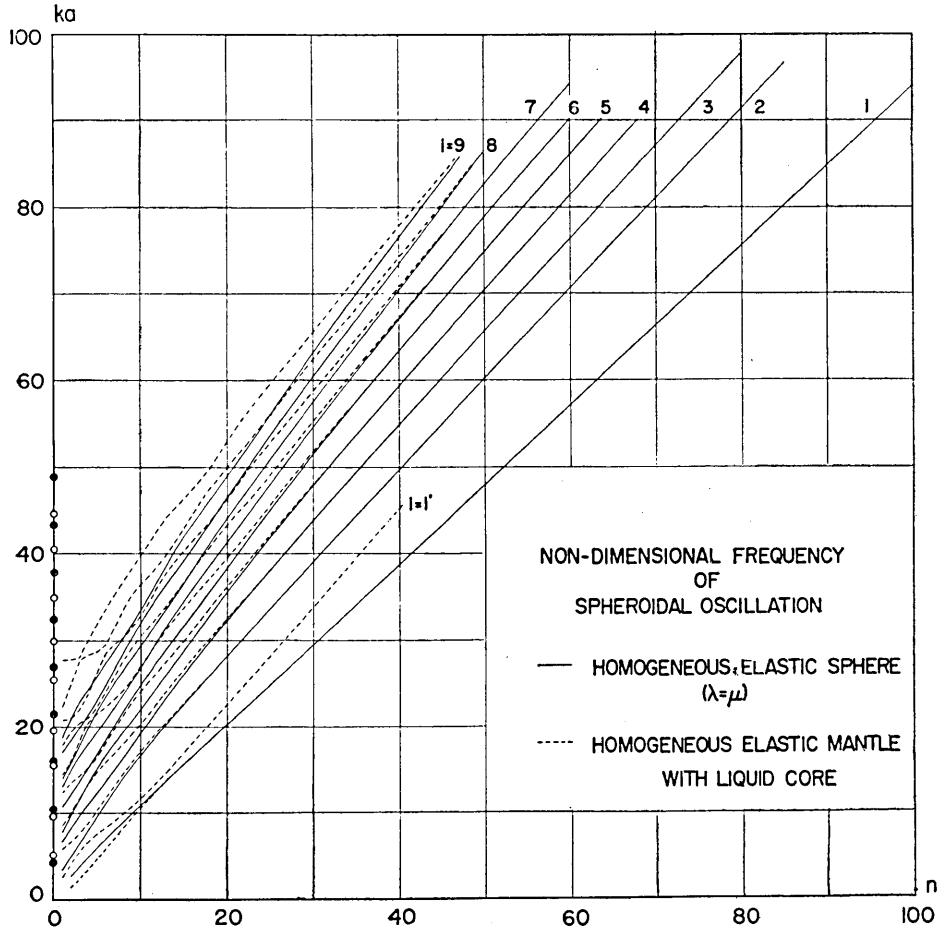

Fig. 1. Non-dimensional frequency ($k_0a=(2\pi a/Vso)/T$) of the free spheroidal oscillation for case II). Vso=shear velocity in the mantle. Broken line and open circle: case II). Solid line and solid circle: case I). $i=1'$ is the special branch which does not exist in case I).

(period axis) and is shown in a rectangular enclosure. By the existence of a liquid core things become complicated and there are minima and maxima in the group velocity curves. Marked difference is found in the group and phase velocity curves of the fundamental mode. They are monotonous for case I), while in the present case II), the phase velocity curve has a maximum and the group velocity changes abruptly at around $n=15$.

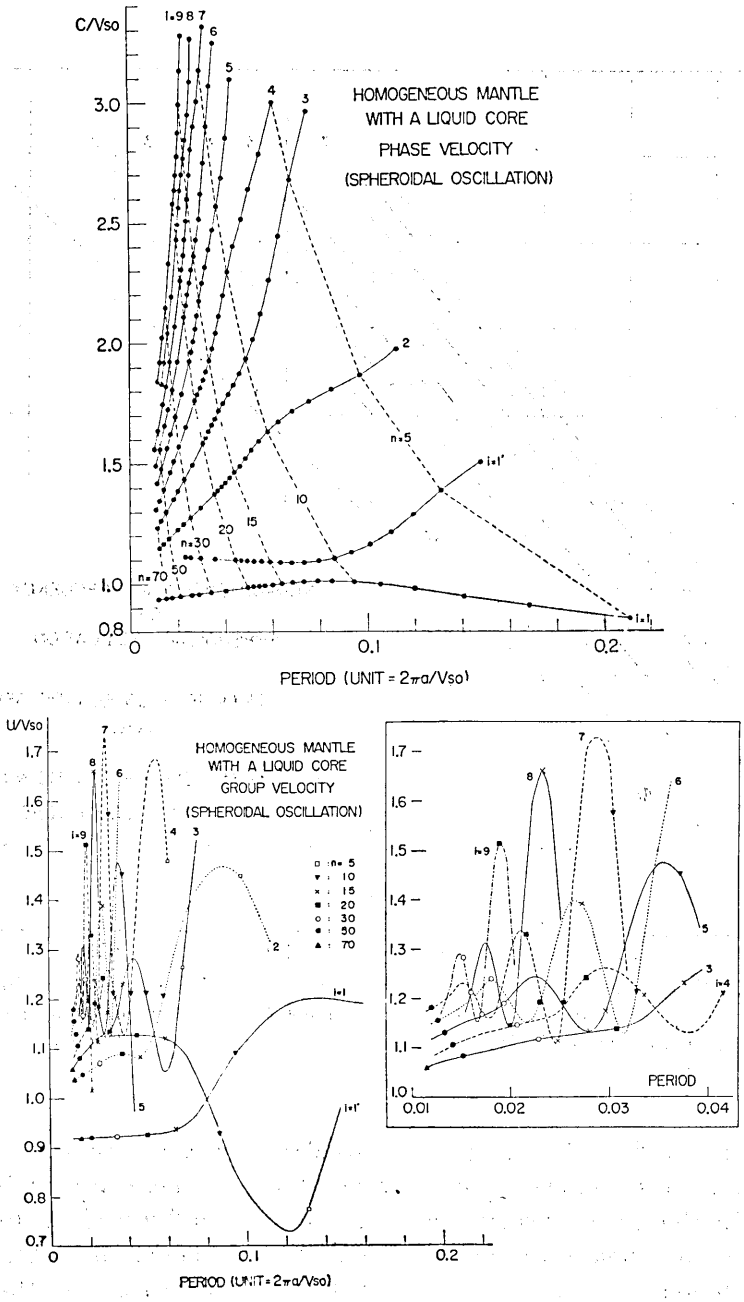

Fig. 2. Phase and group velocity curves as functions of period. In both figures the fundamental mode tends to the corresponding value of plane Rayleigh wave, that is, 0.9194 *Vso*. To show the detailed feature of waves a part of the group velocity figure is enlarged in the direction of period axis and arranged in a rectangular enclosure.

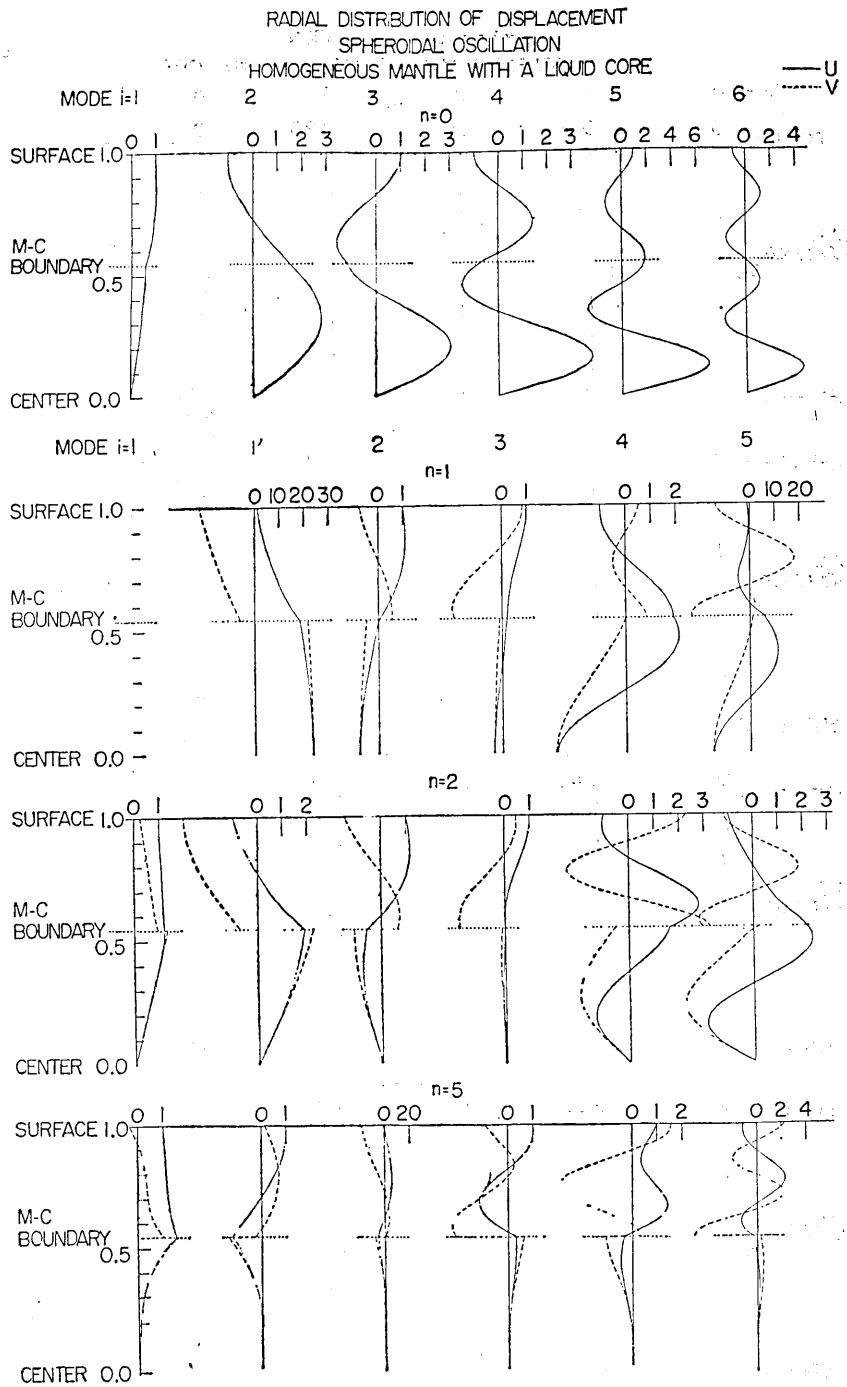
RADIAL DISTRIBUTION OF DISPLACEMENT
SPHEROIDAL OSCILLATION
HOMOGENEOUS MANTLE WITH A LIQUID CORE
U
V
MODE i=1
2
3
4
5
6
n=0
SURFACE 1.0
M-C BOUNDARY
0.5
CENTER 0.0
MODE i=1
1'
2
3
4
5
n=1
SURFACE 1.0
M-C BOUNDARY
0.5
CENTER 0.0
n=2
SURFACE 1.0
M-C BOUNDARY
0.5
CENTER 0.0
n=5
SURFACE 1.0
M-C BOUNDARY
0.5
CENTER 0.0

Fig. 3-1

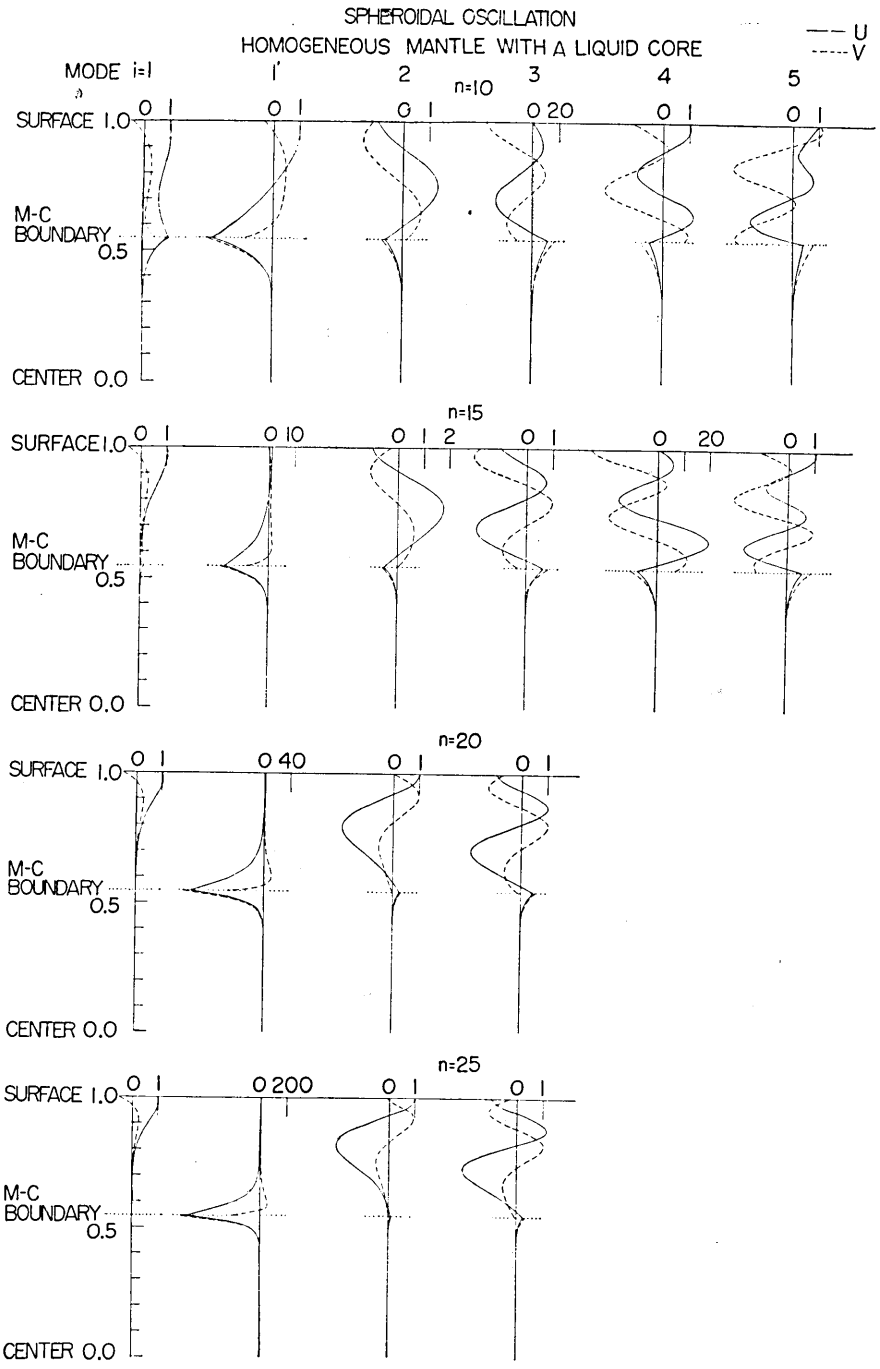
SPHEROIDAL OSCILLATION
HOMOGENEOUS MANTLE WITH A LIQUID CORE
U
V
MODE i=1
1'
2
n=10
3
4
5
SURFACE 1.0
M-C BOUNDARY 0.5
CENTER 0.0
n=15
n=20
n=25

Fig. 3-2

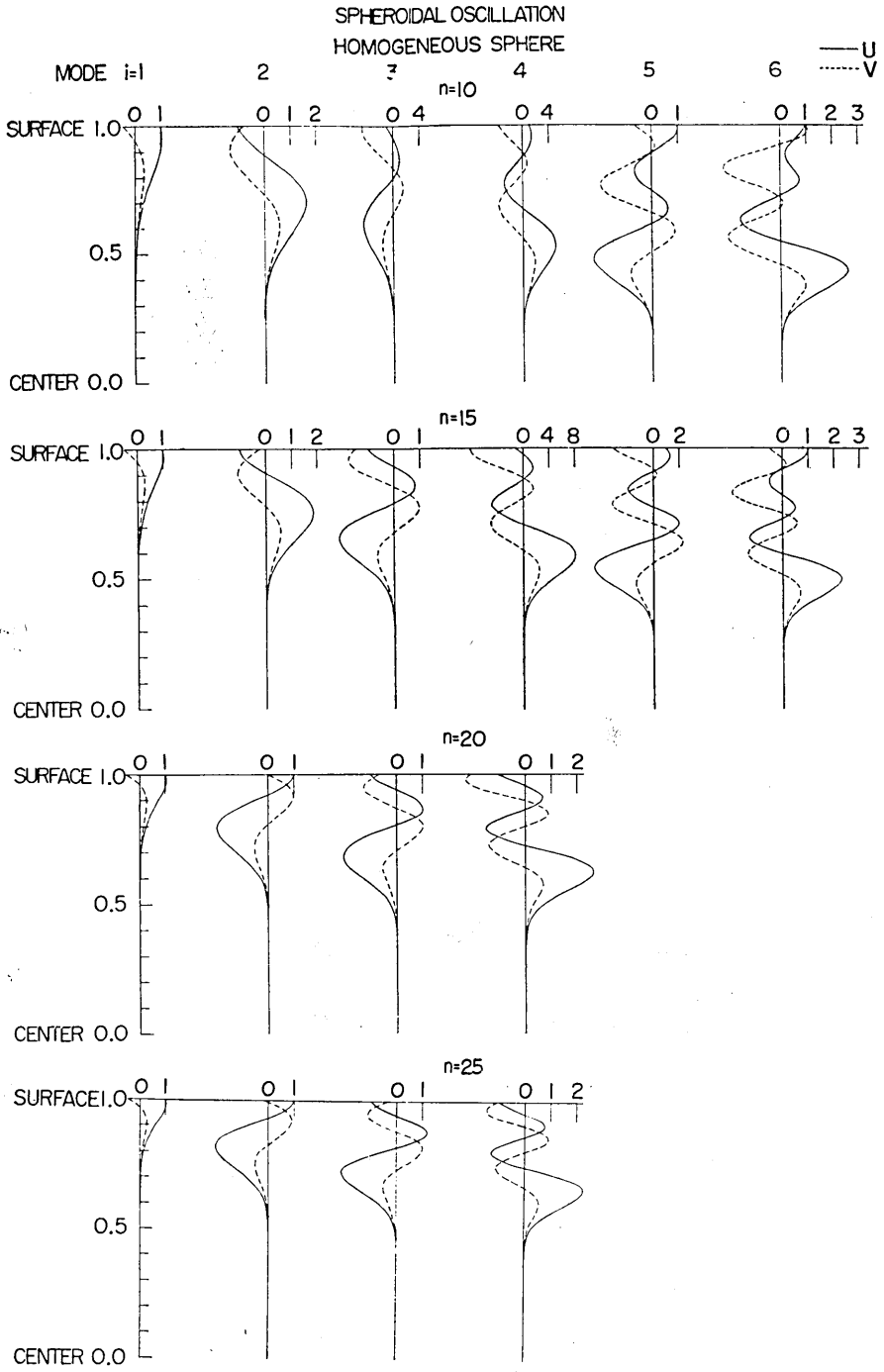

Fig. 3-3

Fig. 3. Radial distribution of displacement. Absolute value of radial displacement on the surface is taken as unit. Solid line: radial displacement $U_n(r)$. Broken line: colatitudinal displacement $nV_n(r)$. (As to the figure of a homogeneous sphere for $n \leqq 5$, refer to our previous paper[5]).

6. Radial distribution of displacements

In order to clarify the nature of the extra branch ($i=1'$), radial distribution of displacements are computed for various values of n and are arranged as in Fig. 3. In this figure, the displacement distribution of normal modes for case I) are also given for reference. Absolute value of the radial displacement on the surface is taken as unit for each mode.

In the extra branch ($i=1'$), the displacements on the core-mantle boundary increase rapidly as n increases, showing the modes as a kind of boundary waves such as Stoneley wave with a plane boundary[4].

$n=1$ is a special mode in which the center of a sphere moves.

7. Common spectrum

Common spectrum ${}_iS_n^u$ is defined by the formula

$$ {}_iS_n^u = C_{mn} \cdot (U_n(r)/dE/dp) \cdot f^*(p), $$

which is a part of the expression in (3.3) and is common in any displacement expressions at various times and locations. Using ${}_iS_n^u$, u is given in the following way.

$$ u = \sum_{i,n} {}_iS_n^u \cdot P_n^m(\cos\theta) \cdot \exp(jpt) , \tag{7.1} $$

Since an axial symmetry is assumed, the azimuthal component w vanishes, the other component v has a similar form

$$ v = \sum_{i,n} {}_iS_n^v \cdot \frac{d}{d\theta} P_n^m(\cos\theta) \cdot \exp(jpt) . \tag{7.2} $$

The common spectrum for u and v is plotted as in Fig. 4.

After passing its maximum, the common spectrum of the branch $i=1'$ decreases rapidly and becomes negligible for $n \geqq 20$. This is consistent with the fact that, as stated in § 6, the branch $i=1'$ shows characters of boundary wave between core and mantle and the amplitude on the boundary is very large compared with that of the surface especially when n is large.

8. Theoretical seismograms.

The geographical distribution of stress on the surface is

$$ \Phi(\theta,\varphi) = \Phi^0(\cos\theta) = \begin{cases} 1 & \theta < \theta_0 \\ 0 & \theta_0 < \theta \end{cases} \qquad (\theta_0 = 0.04 \text{ radian}) $$

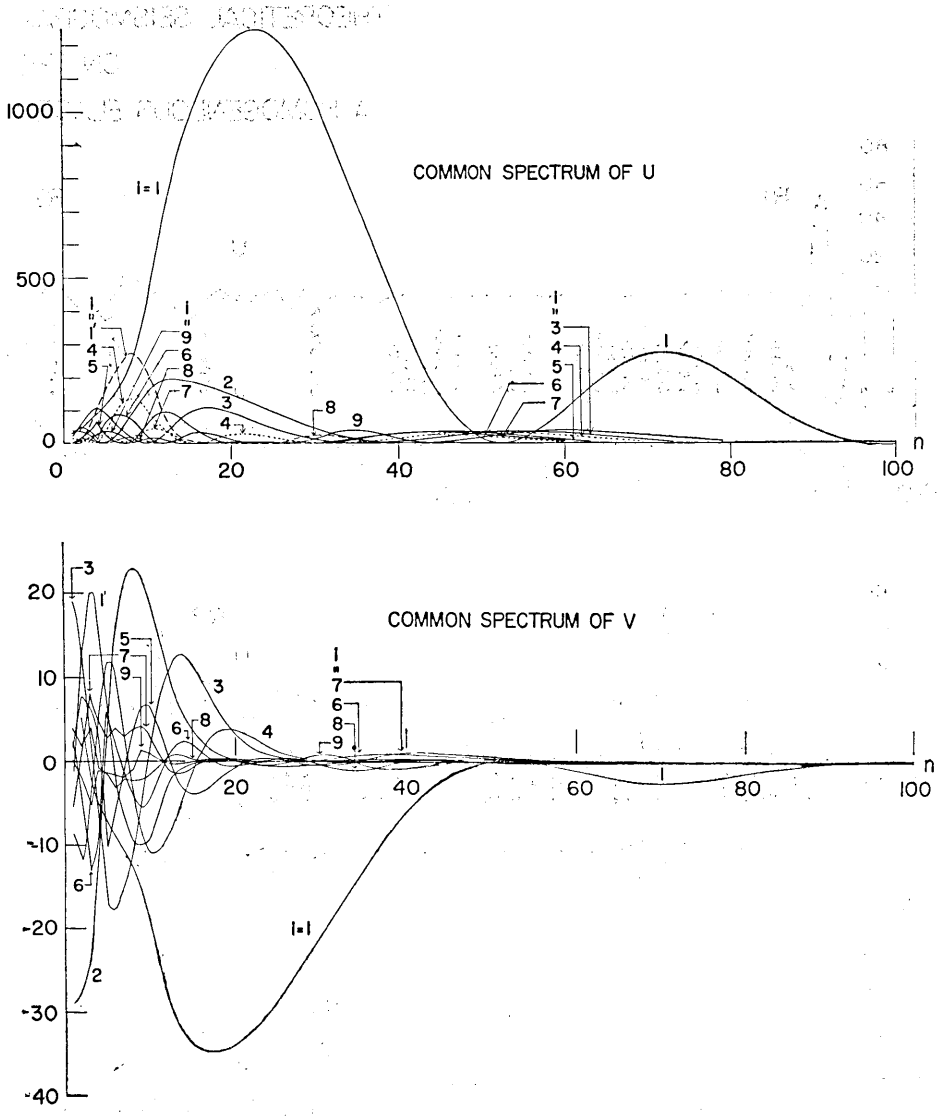

Fig. 4. Common spectrum of radial and colatitudinal components of displacement. Values of radial component for $n=0$, $i=1, 1', \cdots, 9$ are negligible.

and the time distribution is

$$f(t)=\begin{cases}-1 & -t_1<t<0\\ 1 & 0<t<t_1 \quad (t_1=0.02)\\ 0 & |t|>t_1\end{cases}$$

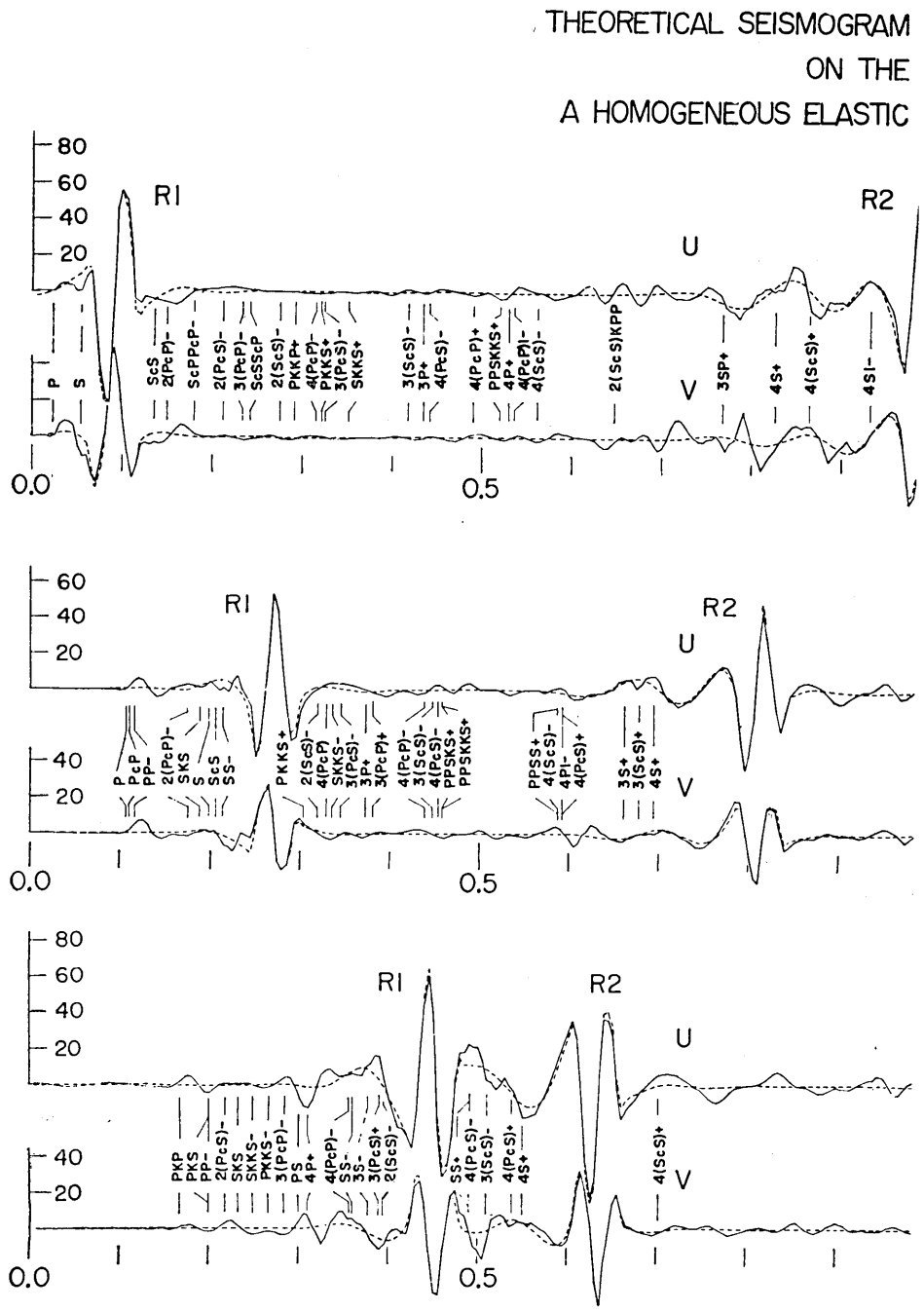

Fig. 5. Theoretical seismogram of spheroidal disturbances on the surface of an various phases of body waves calculated by a simple theory of geometrical optics. Solid line: $({}_9u_{100})$ and $({}_9v_{100})$. Broken line: $({}_1u_{100})$ and $({}_1v_{100})$. Unit of time is $2\pi a/Vso$. to be $2(k+1)r-\theta$ and $k-$ means $2k\pi+\theta$.

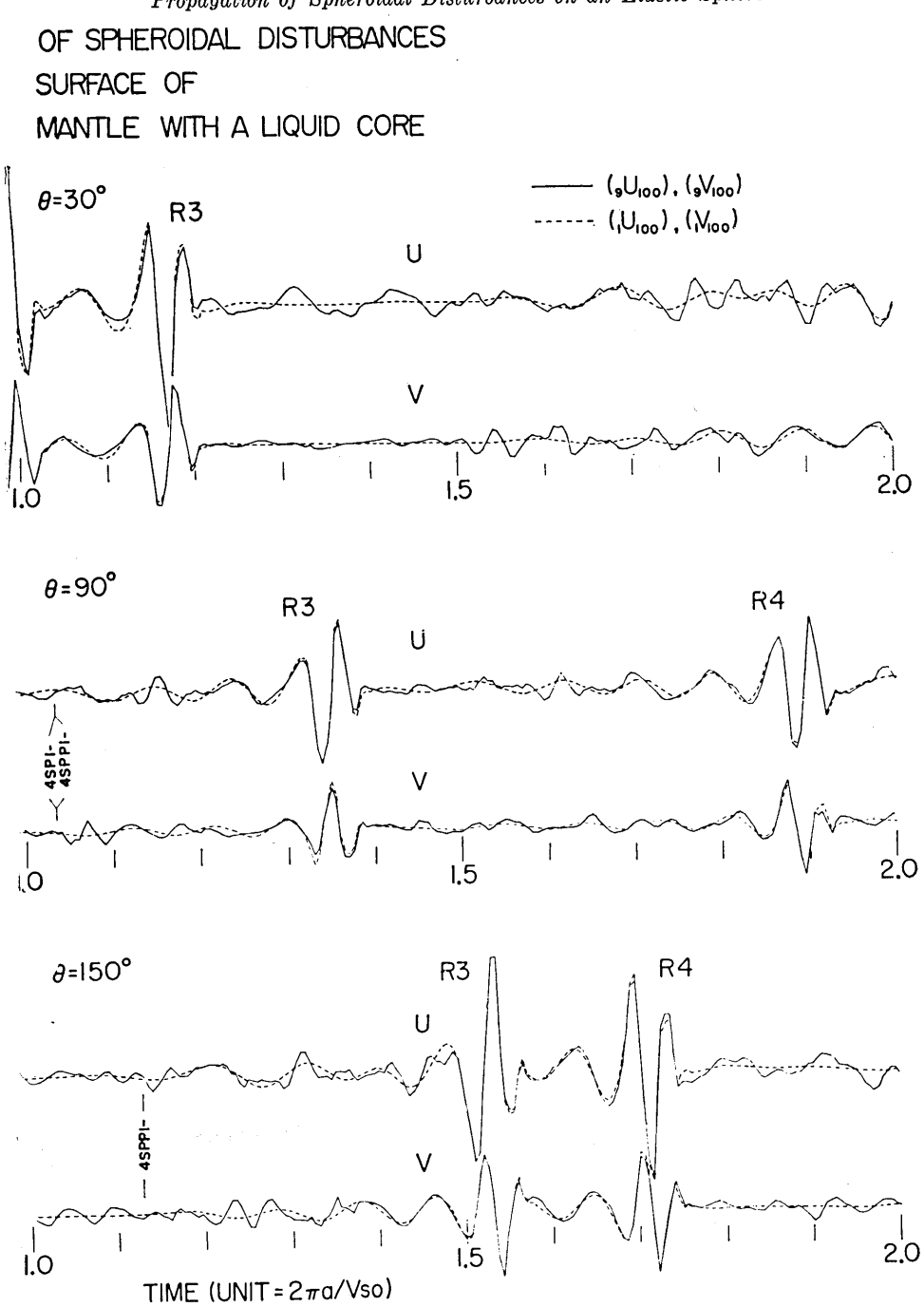

elastic sphere due to a localized force around the pole. Arrows show the arrivals of $k+$ in the end of notations expressing body phases means the epicentral distance

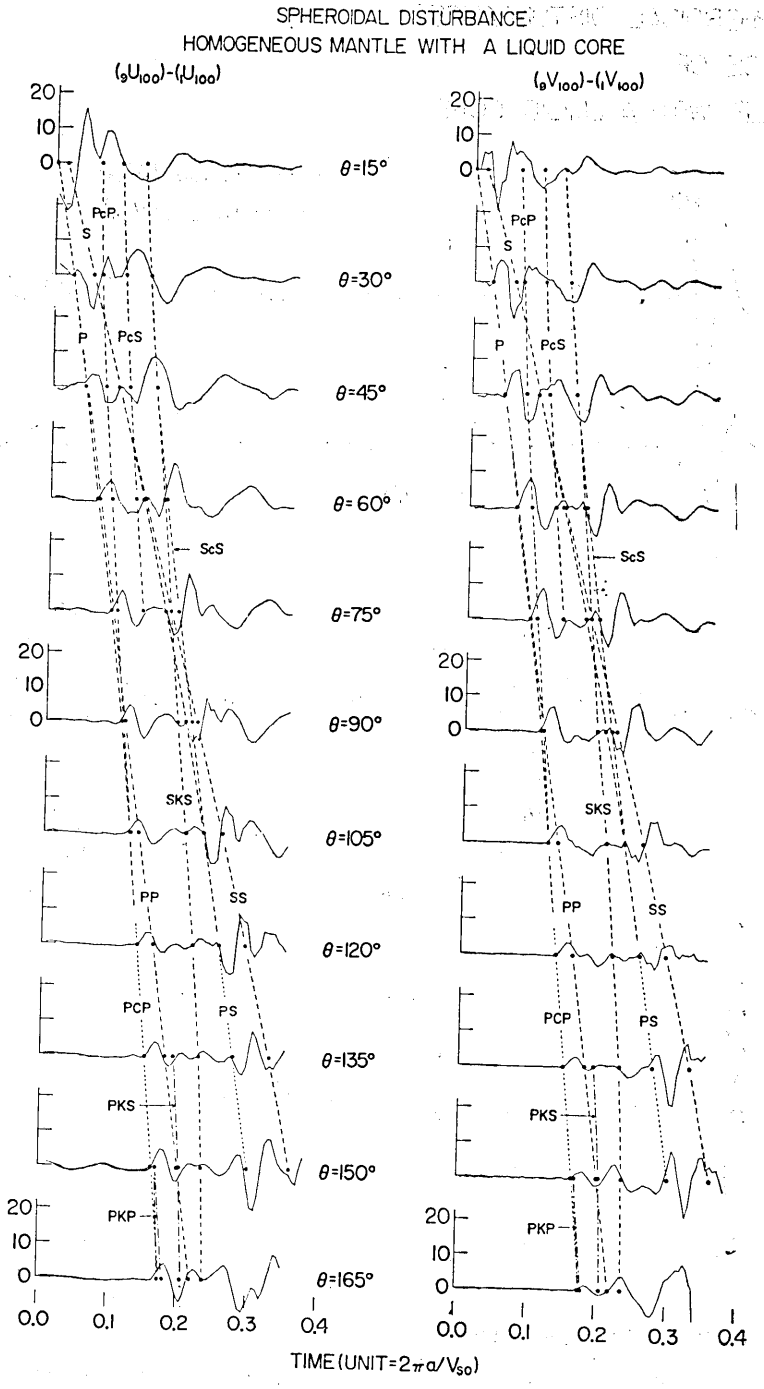

Fig. 6. Radial and colatitudinal displacements computed for various epicentral distances. The curves show contributions of only the higher modes. Solid circles are arrival times of body phases calculated by geometrical optics and broken lines indicate travel time curve of body waves. The wave *PCP* represents *P* wave diffracted by the core in shadow zone.

From the function given above, we have immediately

$$f^*(p) = -4j \sin^2 (pt_1/2)/p \,.$$

Largest values of colatitudinal order number used in the synthesis work can be inferred from the curves in Fig. 4. Beyond those values the amplitude becomes very small and the contribution of those modes are negligible.

Theoretical seismograms are calculated at three points on the surface, namely

$$\theta = 30°,\ 90° \text{ and } 150°.$$

In Fig. 5 the result is shown, in which solid lines refer to $({}_9u_{100})$ and $({}_9v_{100})$, and broken lines $({}_1u_{100})$ and $({}_1v_{100})$.

Direct P and S waves, phases of core and surface reflections, and the transmitted waves through the liquid core are found in the figure. These waves, however, are more clearly identified in the curves consisting of only radial higher modes. Figures are prepared to show the detailed feature of these phases (Fig. 6). The disturbance in the shadow zone is also traced and is expected to provide materials for our future study. The notation PCP was given to this wave, of which amplitudes are shown as a function of epicentral distance in Fig. 7.

As was in the former case I), the fundamental mode (broken line) expresses the surface wave, though it shows a more dispersive character

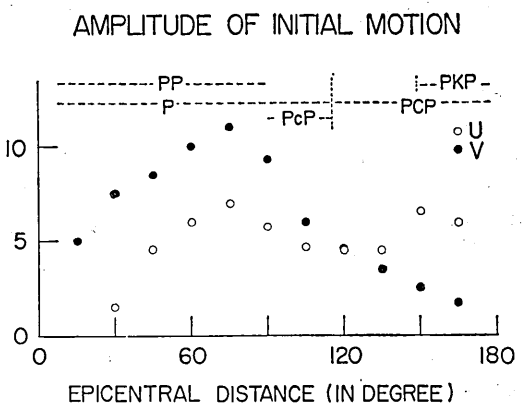

Fig. 7 Amplitude of initial wave as a function of epicentral distance. Open circle: radial displacement. Solid circle: colatitudinal displacement. Name of body phases mean the range in which these waves appear as or immediately after the initial wave.

than the former case. Paying attention to the short period wave, it is found that the broken line ends abruptly at the arrival time of the wave with minimum group velocity, $U=0.9194\,V_{s0}$.

9. Higher modes and body waves.

As is seen from Fig. 2, group velocity curves exceed P wave velocity, $\sqrt{3}\,V_{s0}$ only when $i\geqq 4$. This implies that the displacement

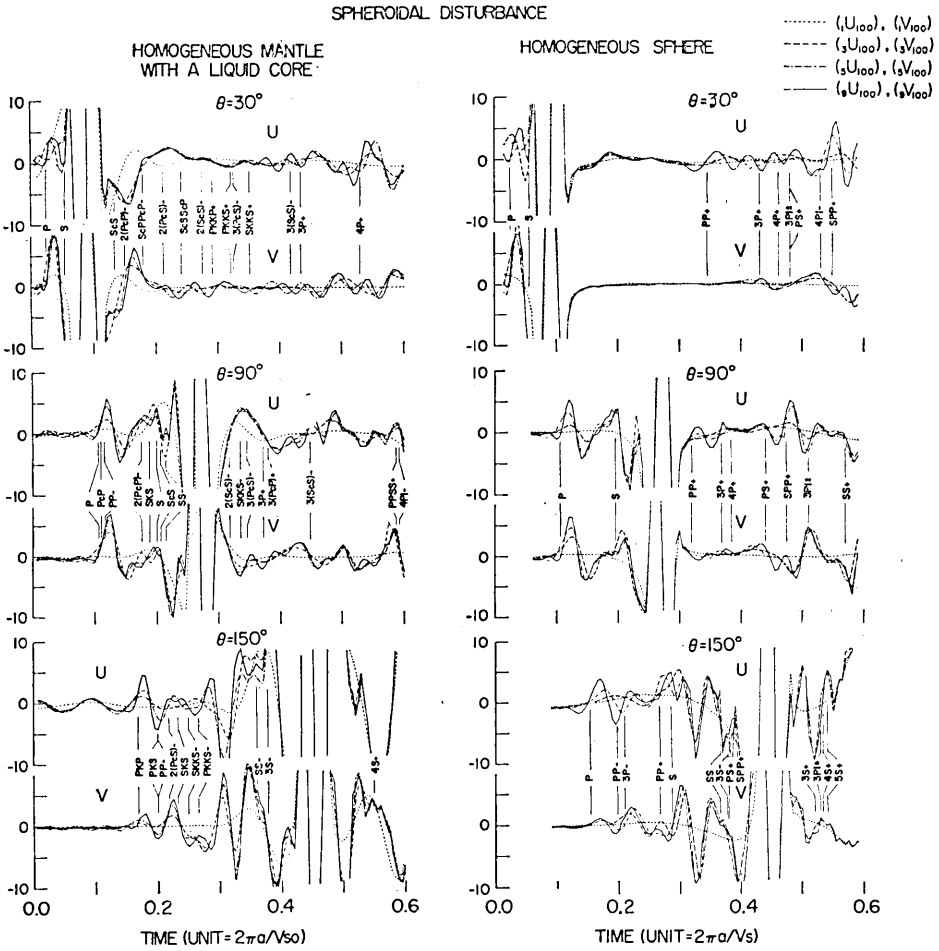

Fig. 8. Theoretical seismogram for the cases I) and II) showing contribution of radial higher modes to various kinds of body waves. Dotted line: $({}_1u_{100})$, $({}_1v_{100})$=contribution of the fundamental mode. Broken line: $({}_3u_{100})$, $({}_3v_{100})$. Chain line: $({}_5u_{100})$, $({}_5v_{100})$. Solid line: $({}_9u_{100})$, $({}_9v_{100})$.

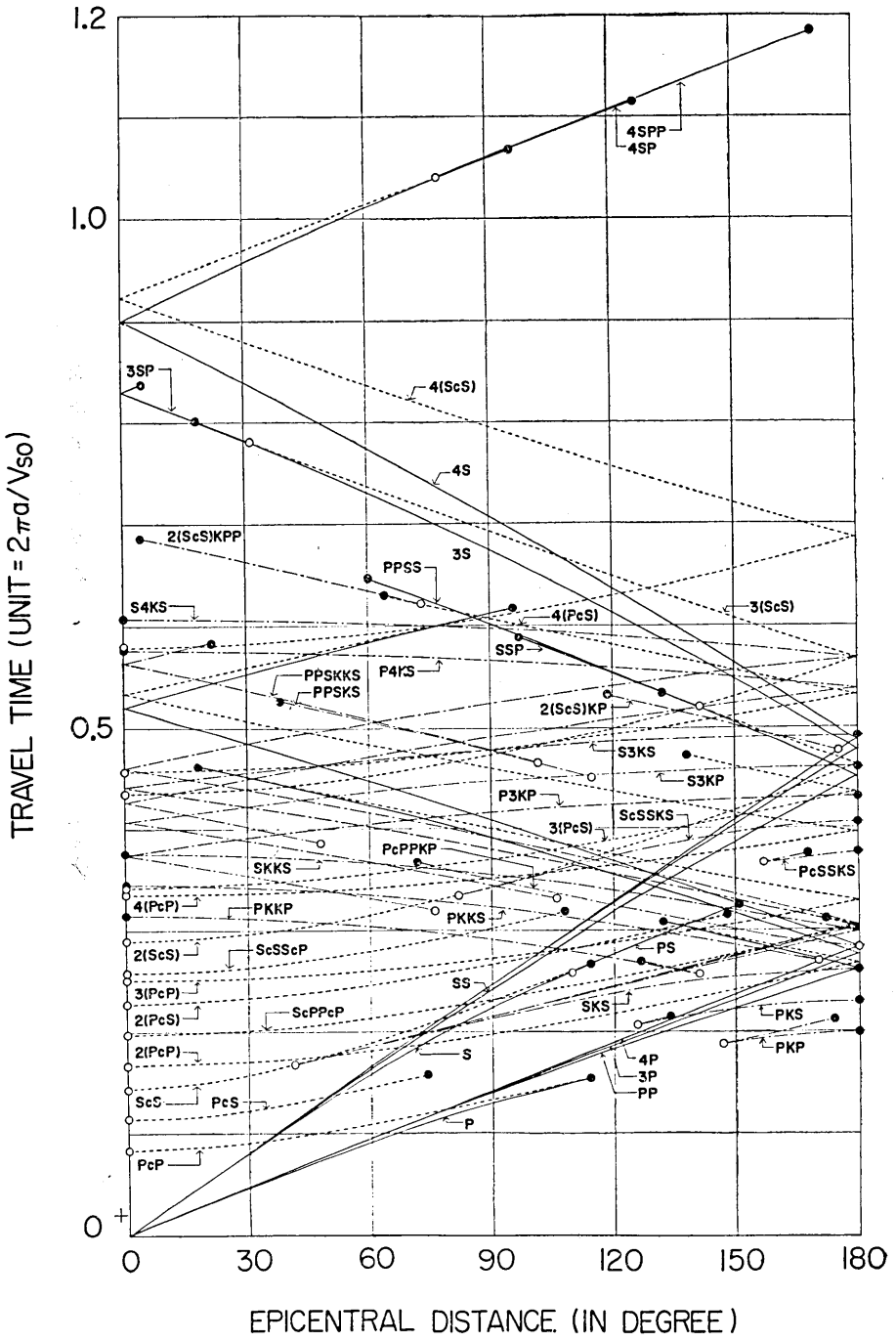

Fig. 9. Travel time curves of various body waves for an impulsive source at the pole. Cross in the lower left is the reference point in the present case. Solid line: direct P and S wave or P and S waves reflected on the surface only. Broken line: waves reflected at the core-mantle boundary. Chain line: waves passed through the core. Open and solid circles show the beginning and end points of various phases respectively.

obtained by summing up the contribution of modes with small values of i (e. g. $i=1, 2, 3$) cannot express the P phase, while S wave can be expressed by the contribution of radial modes of comparatively low order. These disturbances are shown in Fig. 8 which illustrate the above-mentioned characteristics more clearly.

10. Travel time curve.

By a simple theory of geometrical optics the travel time of various phases for an impulsive source at the pole is calculated and is given in Fig. 9. A cross on the lower left of this figure is the reference point for the present case. Open and solid circles represent the points at which certain phases begin and terminate respectively. For example P and S waves end at an epicentral distance $\theta=113.987°$. SP, SSP and SP begin at $\theta=109.5°$, 219.0° and 328.5° respectively. Calculated arrival times are also shown in the theoretical seismogram in Fig. 5 indicated by arrows. The agreement of the expected arrivals and the actual appearance of phases is good.

Acknowledgments

Numerical computations were carried out by an IBM 7090 through the courtesy of the IBM, Japan Ltd. and the Computation Centre, the University of Tokyo, to which our sincere thanks are due.

Reference

1) Y. SATÔ, T. USAMI and M. EWING (1962), "Basic Study on the Oscillation of a Homogeneous Elastic Sphere IV. Propagation of Disturbances on the Sphere." *Geophys. Mag.* **31**, pp. 237-242.

2) Y. SATÔ, T. USAMI, M. LANDISMAN and M. EWING (1963), "Basic Study on the Oscillation of a Sphere V: Propagation of Torsional Disturbances on a Radially Heterogeneous Sphere. Case of a Homogeneous Mantle with a Liquid Core." *Geophys. J.* **8**, pp. 44-63.

3) T. USAMI and Y. SATÔ (1964), "Propagation of Spheroidal Disturbances on a Homogeneous Elastic Sphere." *Bull. Earthq. Res. Inst.* **42**, pp. 273-287.

4) R. STONELEY (1924), "Elastic Waves at the Surface of Separation of Two Solid." *Proc. Roy. Soc. London*, **106**, 416.
Y. SATÔ (1954), "Study on Surface Waves XII. Non-dispersive Surface Waves." *Bull. Earthq. Res. Inst.* **32**, pp. 349-360.
E. STRICK and A. S. GINZBARG (1956), "Stoneley-Wave Velocities for a Fluid-Solid Interface." *B. S. S. A.* **46**, pp. 281-292.
L. E. ALSOP (1963), "Free Spheroidal Vibrations of the Earth at Very Long Periods,

Part I—Calculation of Periods for Several Earth Model." *B. S. S. A.* **53**, pp. 483-502.
5) Y. SATÔ and T. USAMI (1962), "Basic Study on the Oscillation of a Homogeneous Elastic Sphere II. Distribution of Displacement." *Geophys. Mag.* **31**, pp. 25-47.

---

20. 流体核のある等質等方弾性球の表面を伝わるスフェロイド型の振動

地震研究所 佐藤泰夫 宇佐美龍夫

1. 筆者らはさきに，等質等方弾性球を伝わるスフェロイド型の波を，球のいろいろなモードの固有振動の和として表わし，実際の地震記象によく似た理論地震記象を求めた．今回は同様な方法を用い，流体核がある場合の等質等方弾性球の極附近に半径方向の力が加わる場合の変位を，球面上の数点で計算した．

2. まず，固有振動数を求めた．これを各 i に対し n の函数として示すと，等質等方弾性球の $i=1$ と $i=2$ という分枝の間に，特別な分枝 ($i=1'$ と名づける) のあることが分つた．半径方向の振幅分布を計算すると，この枝に属するモードは，核とマントルの境界面で振幅が著しく大きくなる．これは平面境界の場合のストンリー波に似た境界波であることを示す．また一般に固有振動数は n が大きくなると等質等方弾性球の場合に近づく．ついで群速度と位相速度を求めた．これらは前の場合より複雑で群速度には極大，極小が現われた．また，波長が小さくなると位相速度も群速度も等質等方半無限弾性体のレイリー波の速度に近づくこと前回と同様である．また，スペクトルのうち観測点の位置と時刻に無関係な部分 (コモンスペクトル) を求めて図示した．これによると $i=1'$ のスペクトルは $n\geqq 20$ では，ほとんど零となる．

3. 実際の計算にあたつては，軸対称 ($m=0$) を仮定し，また，外力の空間的分布 $\Phi(\theta,\varphi)$，時間的分布 $f(t)$ を次のようにとつた．

$$\Phi(\theta,\varphi)=\begin{cases}1 & \theta<\theta_0\\ 0 & \theta>\theta_0\end{cases} \qquad (\theta_0=0.04 \text{ ラジアン})$$

$$f(t)=\begin{cases}-1 & -t_1<t<0,\\ 1 & 0<t<t_1,\\ 0 & t_1<|t|\end{cases} \qquad (t_1=0.02)$$

時間の単位は (周長)/(マントルの S 波速度) である．ここでは，マントルの S 波速度=6.667 km/sec，マントルの P 波速度=11.55 km/sec，核の P 波速度=10.00 km/sec，核とマントルの密度比=2.2 ととつた．また，地球の半径は 6370 km，マントルの厚さは 2900 km とした．

変位は，時間 $t=0.0$ (0.005) 2.0 について計算し，その結果次のことが分つた．

a) 幾何光学的な考えから求められた実体波の走時は，理論地象記象に見られる各波の発現時とよく一致する．

b) 核での反射波，核内を通過する波，核の陰に表われる回折波が，はつきりわかる．

c) 基本振動は表面波をよく表わしている．表面波は等質等方球の場合より大きな分散性を示す．また，高次の振動は実体波と密接に関係している．この関係を示すために，i の小さい方から 3, 6, 9 個の高次の振動をそれぞれ基準振動に加えた時の振幅を図示した．これによると S 波は低次の高調波で十分よく表わされるが P 波は高次の高調波まで加えなければ表わされないことが分つた．これは低次の振動では群速度が P 波速度に達せず，高次の振動になつて初めて群速度に P 波速度を超える部分が表われることとよく一致する．

d) 群速度に極小値があることに対応し，短周期波に着目すると，表面波の終りの点が，はつきりと理論地象記象上に見い出される．

4. 回折波の振幅を震源距離の関数として図示した．